(a) along and (b) across the tooth length are considered. The paper is supplied with numerical examples.

NOMENCLATURE

$\Delta A^{(i)}$	axial displacement of gear i
b_d	machine setting parameter
$\Delta e^{(i)}$	magnitude of gear eccentricity vector $\Delta \underset{\sim}{e}^{(i)}$ of gear i
ΔE	machine setting
$(\underset{\sim}{i},\underset{\sim}{j},\underset{\sim}{k})$	unit vectors of coordinate system S_f
L	cone distance measured from apex to mean contact point
ΔL	machine setting
$\underset{\sim}{n}$	surface unit normal
(n_x,n_y,n_z)	components of $\underset{\sim}{n}$
q_d	machine setting parameter
$\underset{\sim}{r}$	position vector locating contact point
r_d	mean head cutter radius
$d\underset{\sim}{s}_q^{(i)}$	displacement of contact point due to errors of gear i
S_f	fixed coordinate system
S_d	coordinate system fixed to generating gear
(x,y,z)	components of $\underset{\sim}{r}$
α_1	initial position of eccentricity vector $\Delta \underset{\sim}{e}^{(i)}$
β	gear spiral angle
γ_i	pitch angle of gear i
$\Delta\delta$	sum of gear dedendum angles
Δ_i	dedendum angle of gear i
θ_d	surface coordinate of generating surfaces
Σ_i	surface of gear tooth i

PRECISION OF SPIRAL-BEVEL GEARS

by F. L. Litvin*, R. N. Goldrich+, J. J. Coy**, and E. V. Zaretsky++

National Aeronautics and Space Administration
Lewis Research Center
Cleveland, Ohio 44135

E-1196

SUMMARY

An analytical method was derived for determining the kinematic errors in spiral-bevel gear trains caused by the generation of nonconjugate surfaces, by axial displacements of the gear assembly, and by eccentricity of the assembled gears. Such errors are induced during manufacturing and assembly. Two mathematical models of spiral-bevel gears were included in the investigation. One model corresponded to the motion of the contact ellipse across the tooth surface (geometry I) and the other along the tooth surface (geometry II). The following results were obtained:

1. Kinematic errors induced by errors of manufacture may be minimized by applying special machine settings. The original error may be reduced by an order of magnitude. The procedure is most effective for geometry II gears.

2. When trying to adjust the bearing contact pattern between the gear teeth for geometry I gears, it is more desirable to shim the gear axially; for geometry II gears, shim the pinion axially.

---

* Professor of Mechanical Engineering, University of Illinois at Chicago Circle, Chicago, Illinois 60680; Member ASME.

+ Research Assistant, University of Illinois at Chicago Circle, Chicago, Illinois 60680; Associate Member ASME.

**Propulsion Laboratory, AVRADCOM Research and Technology Laboratories, Lewis Research Center, Cleveland, Ohio 44135; Member ASME.

++ Lewis Research Center, Cleveland, Ohio 44135; Fellow ASME.

3. The kinematic accuracy of spiral-bevel drives are most sensitive to eccentricities of the gear and less sensitive to eccentricities of the pinion. The precision of mounting accuracy and manufacture are most crucial for the gear, and less so for the pinion.

INTRODUCTION

Kinematic errors of spiral bevel gear trains are induced (a) by the applied methods of their generation, and (b) by errors in manufacture and assembly. In practice the generated tooth surfaces are not conjugate and thus result in kinematic errors. To reduce these errors special machine and tool settings must be applied during spiral bevel gear manufacture.

Problems of gear precision were solved by Litvin [1]* and Baxter [2]. Gear-train noise as a result of kinematic errors was investigated by Townsend, Coy, and Hatvani [3].

The new solution to the problem of spiral-bevel gear precision presented in this paper is based on the following principles: (a) the real (nonconjugate) tooth surfaces are replaced by conjugate surfaces; (b) these surfaces are put into mesh by modeling the errors of manufacture and assembly; (c) the influence of these errors on gear-train kinematic errors is studied using the new method of investigation applied in this paper. The investigation of kinematic errors includes (a) the determination of kinematic errors caused by the applied methods of tooth generation, (b) the determination of approximate machine settings used to compensate the kinematic errors resulting from such methods, and (c) the determination of kinematic errors exerted by gear eccentricity and by axial displacements of gears during their assembly. Two models of spiral-bevel geometry [4], corresponding to the contact point path directed

*Numbers in brackets designate References at end of paper.

τ_d see eq. (4)

φ_i angle of rotation of gear i

φ_d angle of rotation of generating gear

$\Delta\varphi_2$ kinematic error function

ψ_c gear pressure angle

METHOD OF INVESTIGATION AND BASIC EQUATIONS

Consider that the contact of gear-tooth surfaces Σ_1 and Σ_2 is localized and that they are in contact at a point at every instant. The location of theoretical contact point M and the direction of the common surface unit normal are given in coordinate system S_f rigidly connected to the frame. The position vector locating the contact point and the unit normal vector are denoted as $\underset{\sim}{r} = \overline{OM}$ and $\underset{\sim}{n}$, respectively. Suppose now that some errors of manufacture and assembly occur. Due to these errors, tooth surfaces Σ_1 and Σ_2 are no longer in tangency - either they interfere with each other or a clearance exists between them (Fig. 1). To bring the two surfaces into tangency, once again, it is sufficient to rotate one of them (the output gear 2) by a small additional angle $\Delta\varphi_2$. The kinematic error function $\Delta\varphi_2$ as a function of gear 1 rotation angle φ_1 may be found by applying the following equation [5]:

$$[\underset{\sim}{\Delta\varphi_2}\underset{\sim\sim}{rn}] = (\Sigma\underset{\sim}{ds}_q^{(1)} - \Sigma\underset{\sim}{ds}_q^{(2)}) \cdot \underset{\sim}{n} \qquad (1)$$

Here, $\Sigma\underset{\sim}{ds}_q^{(i)}$ represent small changes in the position of the contact point due to errors of manufacture and assembly of gear "i" (where i = 1,2).

Equation (1) is applied to two spiral-bevel geometries. Geometry I corresponds to the contact point path running across the length of the gear teeth (Fig. 2(a)). Gears with this geometry are generated using two tool cones (generating surfaces) which are rigidly connected and in tangency along

a common cone genatrix, line L (Fig. 2(b)). In the process of meshing, the contact point moves through space along line L. Geometry II corresponds to the contact point path running along the length of the gear teeth (Fig. 3(a)). These gears are generated by tool surfaces which are a cone and a surface of revolution which are in tangency along a circle L (Fig. 3(b)). In the process of meshing the contact point moves through space along circle L. Figures 4 and 5 show the coordinate systems applied to express the equations for the contact point path and surface unit normal vectors for both geometry I and geometry II gears. Coordinate system S_f is rigidly connected to the frame and system S_d is rigidly connected to the generating gear. Auxiliary coordinate system S_c (Fig. 5) is also rigidly connected to the generating gear (and to system S_d).

Expression of the equations is based on the following principles [1]: (a) Two generating surfaces are rigidly connected and in tangency along a line L. These surfaces form the two generating gears - surface Σ_A generates gear 1 and surface Σ_B generates gear 2. (b) The four gears that are in mesh - the two generating gears and the two generated gears - all have the same instantaneous axis of rotation, axis z_f. (c) Generated surfaces Σ_1 and Σ_2 always contact each other at a point that belongs to line L, while their common normal intersects axis z_f, the instantaneous axis of rotation. (d) The line of action is the locus of contact points (contact point path) of surfaces Σ_1 and Σ_2 represented in coordinate system S_f.

On the basis of the above principles, there results the following equations for the position vector $r(\varphi_d)$ of a point on the line of action (contact point path) and the surface unit normal $\underset{\sim}{n}(\varphi_d)$:

$$\underset{\sim}{r}(\varphi_d) = x(\varphi_d)\underset{\sim}{i} + y(\varphi_d)\underset{\sim}{j} + z(\varphi_d)\underset{\sim}{k}$$

$$\underset{\sim}{n}(\varphi_d) = n_x(\varphi_d)\underset{\sim}{i} + n_y(\varphi_d)\underset{\sim}{j} + n_z(\varphi_d)\underset{\sim}{k}$$

Here φ_d is the angle of rotation of the generating gear.

For Geometry I:

$$\left.\begin{aligned} x &= r_d - b_d \frac{\sin(q_d - \varphi_d)}{\sin \tau_d} \sin_c\Psi \cos_c\Psi \\ y &= \frac{\sin \tau_d}{\tan \Psi_c} x \\ z &= \frac{b_d \sin \Theta_d}{\sin \tau_d} + \frac{\cos \tau_d}{\tan \Psi_c} x \end{aligned}\right\} \quad (2)$$

$$\left.\begin{aligned} n_x &= \sin \Psi_c \\ n_y &= \cos \Psi_c \sin \tau_d \\ n_z &= \cos \Psi_c \cos \tau_d \end{aligned}\right\} \quad (3)$$

$$\tau_d = \Theta_d - q_d + \varphi_d; \quad \Theta_d - q_d = 90^\circ - \beta \quad (4)$$

Here, Ψ_c is the gear pressure angle; q_d and $b_d = O_f O_c$ are parameters of machine settings; $r_d = O_c M$ is the mean head cutter radius; β is the gear spiral angle.

For Geometry II:

$$\left.\begin{aligned} x &= 0 \\ y &= 0 \\ z &= r_d \cos \tau_d + b_d \cos(q_d - \varphi_d) \end{aligned}\right\} \quad (5)$$

$$\left.\begin{aligned} n_x &= \sin \Psi_c \\ n_y &= \cos \Psi_c \sin \tau_d \\ n_z &= \cos \Psi_c \cos \tau_d \end{aligned}\right\} \quad (6)$$

Here $\phi_d \neq$ constant, and ϕ_d and φ_d are related by

$$r_d \sin \tau_d - b_d \sin(q_d - \varphi_d) = 0 \qquad (7)$$

The line of action of Geometry II gears coincides with axis z_f.

EVALUATION OF KINEMATIC ERROR FUNCTIONS

For most gears, kinematic error functions $\Delta\varphi_2(\varphi_d)$ (defined by eq. (1))are piecewise (noncontinuous) functions with discontinuities at the points of changing gear teeth. To evaluate these functions one must examine (a) the range of the kinematic error function over the mesh of one gear tooth, and (b) the size of the jump at the points of function discontinuities. Note that the magnitudes of the error functions are of secondary importance - more important are the changes in these functions which are given by (a) and (b) above. Large changes and jumps in kinematic error functions are a source of excessive tooth surface wear, vibrations, noise, and the impact loading of gear teeth. Because of these maladies it is important to understand and evaluate the nature of the kinematic errors caused by gear manufacture and different types of mounting errors.

To apply the general equation (1), a sample gearset was chosen as follows:

N_1 no teeth gear 1 = 20

N_2 no teeth gear 2 = 40

M_{12} $\omega_1/\omega_2 = 2.0$

Σ shaft angle = 90°

ψ_c pressure angle = 20°

β mean spiral angle = 35°

L cone distance - apex-to-main contact point = 4 in.

r_A mean radius of head cutter for Σ_A = 4 in.

q_A (see Fig. 5) = 62.5°

b_A (see Fig. 5) = 3.6939 in.

γ_1 pitch angle gear 1 = 26.57°

γ_2 pitch angle gear 2 = 63.43°

Angle of rotation for one tooth of gear 1: $-9^\circ \leq \varphi_1 \leq 9^\circ$

Kinematic Errors Due to Methods of Tooth Generation

Consider Figs. 4 and 5. Conjugate gear tooth surfaces may be generated if axis-x_f is the common axis of rotation of the generating surfaces, and if axis-z_f is the instantaneous axis of rotation belonging to both the generating surfaces and the generated tooth surfaces. In practice, when generating gears 1 and 2, the axes of rotation of the generating surfaces make angles of Δ_1 and Δ_2, respectively, with axis x_f (Fig. 6). Here Δ_i $(i = 1,2)$ are the dedendum angles of the respective gears. To simulate these manufacturing errors, rotate the generating surface of gear 1 (with respect to that of gear 2) by an amount

$$\underset{\sim}{\Delta\delta} = \Delta\delta\underset{\sim}{j} = (\Delta_1 + \Delta_2)\underset{\sim}{j} \tag{8}$$

Therefore the displacement of the theoretical contact point due to errors may be represented as

$$\underset{\sim}{ds_q^{(1)}} = \underset{\sim}{\Delta\delta} \times \underset{\sim}{r} = \underset{\sim}{\Delta\delta} \times (z\underset{\sim}{i} - x\underset{\sim}{k}) \tag{9}$$

Then, from equations (7) and (1)

$$\Delta\varphi_2(\varphi_d) = \frac{(zn_x - xn_z)\Delta\delta}{-y\cos\gamma_2 n_x + (x\cos\gamma_2 + z\sin\gamma_2)n_y - y\sin\gamma_2 n_z} \tag{10}$$

Here $\varphi_d = \varphi_1 \sin\gamma_1$; γ_2 is the pitch angle of gear 2. This equation was applied to the example gearset with approximate dedendum angles calculated by

$$\tan \Delta_i = \frac{2.5 \sin \gamma_i}{N}$$

resulting in

$$\Delta\delta = \Delta_1 + \Delta_2 = 0.0559 + 0.0558 = 0.1117 \text{ rad}$$

Fig. 7 shows the plot of $\Delta\varphi_2$ vs. φ_1 due to errors of manufacture for both geometry I and geometry II. Both curves are nearly linear but with opposite slopes. During the mesh of one pinion tooth the kinematic error function changes by approximately 14 to 19 arc-minutes. Now the objective is to minimize these kinematic errors by applying special machine settings. These machine settings are represented by translating the pinion (gear 1) by the amount

$$\Delta \underset{\sim}{s}_q^{(1)} = \Delta E \underset{\sim}{j} + \Delta L \underset{\sim}{k} \tag{11}$$

This yields that the total kinematic error function due to $\Delta\delta$, ΔE, and ΔL is given by

$$\Delta\varphi_2(\varphi_d) = \frac{\Delta E n_y + \Delta L n_z - (z n_x - x n_z)\Delta\delta}{-y \cos \gamma_2 n_x + (x \cos \gamma_2 + z \sin \gamma_2) n_y - y \sin \gamma_2 n_z} \tag{12}$$

To find the appropriate values of ΔE and ΔL, two conditions are imposed on equation (12):

$$\Delta\varphi_2 = 0 \tag{13}$$

$$\frac{d(\Delta\varphi_2)}{d\varphi_1} = 0 \tag{14}$$

at the "midpoint" of gear tooth 1 rotation, $\varphi_1 = 0$. Applying equations (12) to (14) and (2) to (7) results in

Geometry I:

$$\frac{\Delta E}{L} = \frac{\tan \psi_c \cos 2\beta}{\cos \beta} \Delta\delta \tag{15}$$

$$\frac{\Delta L}{L} = 2 \tan \psi_c \sin \beta \, \Delta\delta \tag{16}$$

Geometry II:

$$\frac{\Delta E}{L} = (\cos \beta - \sin \beta \tan q_d)\tan \psi_c \, \Delta\delta \tag{17}$$

$$\frac{\Delta L}{L} = (\sin \beta + \cos \beta \tan q_d)\tan \psi_c \, \Delta\delta \tag{18}$$

For the example gearset

Geometry I:

$\Delta E = 0.0679$ in.

$\Delta L = 0.1866$ in.

Geometry II:

$\Delta E = -0.0460$ in.

$\Delta L = 0.3492$ in.

The plot of kinematic errors <u>after</u> the application of machine settings is shown in Fig. 8. As may be observed the $\Delta\varphi_2$ function is now of near-parabolic shape and the range of the original error function is reduced between 10 and 15 times. Since the range of error is smaller for gears of geometry II, it is concluded that compensating for errors by adjusting machine settings is most effective for gears of geometry II. Thus the application of special machine settings is very effective in the reduction of the kinematic errors caused by the method of generation applied in practice. Fig. 9 shows the kinematic error function $\Delta\varphi_2(\varphi_1)$ plotted over the mesh of several gear teeth. Notice that, at the points of changing gear teeth, there is no jump in the value of this function. However, there are discontinuities in its slope.

Kinematic Errors Due to Axial Displacements of Gears

In practice, during the mounting of spiral-bevel gears and during their testing on Gleason Works machines, it is common to change their axial positions in order to correct the location and size of the bearing contact pattern between the gear teeth [6]. Such axial displacements can induce kinematic errors in the gear train which remain unnoticed unless the relations between the angles of gear rotation are examined. It is for this reason that it is important to investigate the nature of kinematic errors which accompany such mounting changes.

Changes in the axial position of gear "i" are represented by vectors $\Delta\underset{\sim}{A}^{(i)}$ ($i = 1,2$). Vectors $\Delta\underset{\sim}{A}^{(i)}$ point <u>out</u> from the apex of their respective pitch cones. The kinematic error function for this case is given by

$$\Delta\phi_2(\phi_1) = \frac{(\Delta A^{(1)} \sin\gamma_1 + \Delta A^{(2)} \sin\gamma_2)n_x + (\Delta A^{(1)} \cos\gamma_1 - \Delta A^{(2)} \cos\gamma_2)n_x}{-(y \cos\gamma_2)n_x + (x \cos\gamma_2 + z \sin\gamma_2)n_y - (y \sin\gamma_2)n_z} \tag{19}$$

The kinematic error functions which are induced by axial displacements of the pinion and gear (gear 1 and 2, respectively) are shown in Fig. 10. Taking into account that the main criterion for evaluating a kinematic error function is not so much its magnitude, but rather, the amount it changes during the mesh cycle, the following conclusion is true for the example gearset: When trying to improve the bearing contact for geometry I gears it is more desirable to displace the <u>gear</u> axially; for geometry II gears it is more desirable to displace the <u>pinion</u> axially.

Kinematic Errors Due to Gear Eccentricities

A gear is said to be eccentric when its geometric axis (the axis about which it rotates during cutting) does not coincide with its axis of rotation

during operation. Gear eccentricity may be induced both by errors of manufacture and assembly. Denoting the magnitudes of gear eccentricities by $\Delta e^{(i)}$ $(i = 1,2)$, the displacement of the contact point is given by the vectors $\Delta\underline{e}^{(1)}$ which rotate about gear axis "i". Further, the original position of the eccentricity vector is given by angles $\alpha_i (i = 1,2)$. Applying equation (1) results in

$$\Delta\varphi_i(\varphi_d) = \frac{n_x \Sigma\Delta e_x + n_y \Sigma\Delta e_y + n_z \Sigma\Delta e_z}{-(y\cos\gamma_2)n_x + (x\cos\gamma_2 + z\sin\gamma_2)n_y - (y\sin\gamma_2)n_z} \tag{20}$$

where

$$\Sigma\Delta e = \Delta e_k^{(1)} - \Delta e_k^{(2)};\ (k = x,y,z)$$

and

$$\left.\begin{aligned} \Sigma\Delta e_x &= \Delta e_1 \cos(\varphi_1 + \alpha_1)\cos\gamma_1 - \Delta e_2 \cos(\varphi_2 + \alpha_2)\cos\gamma_2 \\ \Sigma\Delta e_y &= -\Delta e_1 \sin(\varphi_1 + \alpha_1) - \Delta e_2 \sin(\varphi_2 + \alpha_2) \\ \Sigma\Delta e_z &= -\Delta e_1 \cos(\varphi_1 + \alpha_1)\sin\gamma_1 - \Delta e_2 \cos(\varphi_1 + \alpha_1)\sin\gamma_2 \end{aligned}\right\} \tag{21}$$

To simplify expressions (20) and (21), one may approximate by considering the angle of rotation of the generating gear for one tooth as small: $\varphi_1 \sin\gamma_1 \simeq 0$ so that the kinematic error function is now given by

$$\Delta\varphi_2(\varphi_1) = \frac{a_1 \sin(\varphi_1 + \alpha_1) + b_1 \cos(\varphi_1 + \alpha_1) + a_2 \sin(\varphi_2 + \alpha_2) + b_2 \cos(\varphi_2 + \alpha_2)}{L \sin\gamma_2 \cos\nu_c \cos\beta} \tag{22}$$

where

$$\varphi_2 = \frac{N_1}{N_2}\varphi_1$$

$$a_1 = -\Delta e_1 \cos \psi_c \cos \beta;\ b_1 = \Delta e_1 (\cos \gamma_1 \sin \psi_c - \sin \gamma_1 \cos \psi_c \sin \beta)$$

$$a_2 = -\Delta e_2 \cos \psi_c \cos \beta;\ b_2 = -\Delta e_2 (\cos \gamma_2 \sin \psi_c + \sin \gamma_2 \cos \psi_c \sin \beta) \qquad (23)$$

Unlike the case of spur gears [5] the actual kinematic error function (eq. (20)) has discontinuities at the points where gear teeth change during meshing. However, the overall shape of this function is given by equation (22). This approximate function is a sum of four harmonics: The period of two of them coincides with the period of revolution of gear 1, and two of them with the period of revolution of gear 2. Figure 11 shows the results of plotting functions (20) and (22) for both geometry I and geometry II gears. Here

$$\Delta e_1 = 0.002 \text{ in.} \qquad \alpha_1 = \alpha_2 = 0^\circ$$
$$\Delta e_2 = 0.0 \text{ in.}$$

Figure 12 shows the smooth kinematic error function for

$$\Delta e_1 = 0.002 \text{ in.} \qquad \alpha_1 = 0^\circ$$
$$\Delta e_2 = 0.002 \text{ in.} \qquad \alpha_2 = 180^\circ$$

It is clear that the angle of the gear "contribution" to the kinematic error function is somewhat larger than the pinion contribution. Thus, in general, the bearings and overall mounting precision of the gear are more crucial to spiral-bevel gear-drive accuracy than those of the pinion.

The calculations for the examples presented in the paper are summarized in the Appendix.

SUMMARY OF RESULTS

An analytical method was derived for determining the kinematic errors in spiral-bevel gear trains caused by the generation of nonconjugate surfaces, by

axial displacements of the gear assembly, and by eccentricity of the assembled gears. Such errors are induced during manufacturing and assembly. Two mathematical models of spiral-bevel gears were included in the investigation. One model corresponded to the motion of the contact ellipse across the tooth surface (geometry I) and the other along the tooth surface (geometry II). The following results were obtained:

1. Kinematic errors induced by errors of manufacture may be minimized by applying special machine settings. The original error may be reduced by an order of magnitude. The procedure is most effective for geometry II gears.

2. When trying to adjust the bearing contact pattern between the gear teeth for geometry I gears, it is more desirable to shim the gear axially; for geometry II gears, shim the pinion axially.

3. The kinematic accuracy of spiral-bevel drives are most sensitive to eccentricities of the gear and less sensitive to eccentricities of the pinion. The precision of mounting accuracy and manufacture are most crucial for the gear, and less so for the pinion.

APPENDIX - SUMMARY OF EXAMPLE CALCULATIONS

Symbol	Definition	Value
N_1	Number of pinion teeth	20
N_2	Number of gear teeth	40
M_{12}	Angular velocity ratio = N_2/N_1	2
Σ	Shaft angle	90°
Ψ_c	Pressure angle	20°
β	Mean spiral angle	35°
L	Cone distance - apex to main contact point	4 in.
r_A	Mean head cutter radius for pinion	4 in.
q_A	Machine setting (see Fig. 5(c))	62.5°
b_A	Machine setting (see Fig. 5(c))	3.6939 in.
γ_1	Pitch angle of pinion	26.57°
γ_2	Pitch angle of gear	63.43°
Δ_1	Dedendum angle of pinion	0.0559 rad.
Δ_2	Dedendum angle of gear	0.0558 rad.

To obtain the kinematic error functions, the formulas defining them must be evaluated for different values of φ_1 corresponding to the rotation of the pinion. For kinematic errors caused by methods of tooth generation and by axial displacements the period of the kinematic error function is equal to the pitch angle of the pinion. For errors caused by gear eccentricity the error function has a period which depends on the angular velocity ratio M_{12} (see ref. [5]).

Range of pinion rotation

$$\frac{-360^\circ}{2N_1} \le \varphi_1 \le \frac{360^\circ}{2N_1} \qquad -9^\circ \le \varphi_1 \le 9^\circ$$

All kinematic error functions are evaluated here for

$$\varphi_1 = 3^\circ$$

$$\varphi_A = \varphi_1 \sin \gamma_1 = 1.3419^\circ$$

$$\theta_A = \begin{cases} \text{Geom I: } 90 + q_A - \beta \\ \text{Geom II: } \sin^{-1} \dfrac{b_A \sin(q_A - \varphi_A)}{r_A} + q_A - \varphi_A \end{cases} \quad \begin{matrix} \text{Geom I: } 117.5^\circ \\ \text{Geom II: } 115.15^\circ \end{matrix}$$

$$\tau_A = \theta_A - q_A + \varphi_A \qquad \begin{matrix} \text{Geom I: } 56.34^\circ \\ \text{Geom II: } 53.99^\circ \end{matrix}$$

Contact Point and Unit Normal

$$\begin{Bmatrix} x \\ y \\ z \end{Bmatrix} \text{ Geom I: eqs. (2) } \begin{Bmatrix} 0.03620 \\ 0.08285 \\ 3.99 \end{Bmatrix} \text{in.} \qquad \text{Geom II: eqs. (5) } \begin{Bmatrix} 0.0 \\ 0.0 \\ 4.1336 \end{Bmatrix} \text{ in.}$$

$$\begin{Bmatrix} n_x \\ n_y \\ n_x \end{Bmatrix} \text{Geom I: eqs. (3) } \begin{Bmatrix} 0.3420 \\ 0.7822 \\ 0.5208 \end{Bmatrix} \text{ in.} \qquad \text{Geom II: eqs. (6) } \begin{Bmatrix} 0.3420 \\ 0.7601 \\ 0.5525 \end{Bmatrix} \text{ in.}$$

Kinematic Errors Due to Methods of Tooth Generation

$$\Delta\delta = \Delta_1 + \Delta_2 \qquad 0.1117 \text{ rad}$$

Before machine settings (see Fig. 7)

$\Delta\varphi_2$ eq. (10) Geom I: $-3^\circ\ 7'\ 43''$

Geom II: $-3^\circ\ 13'\ 11''$

Machine settings

Geom I:	ΔE	eq. (15)	0.0679 in.
	ΔL	eq. (16)	0.1866 in.
Geom II:	ΔE	eq. (17)	-0.0460 in.
	ΔL	eq. (18)	0.3492 in.

After machine settings (see Fig. 8)

$\Delta\varphi_2$ eq. (12) Geom I: -6"

Geom II: 4"

Kinematic Errors Due to Axial Displacements

Pinion only (see Fig. 10(a)):

Given $\Delta A^{(1)} = 0.20$ in. $\Delta A^{(2)} = 0$

$\Delta\varphi_2$ eq. (19) Geom I: 2° 34' 30"

Geom II: 2° 38' 20"

Gear only: (see Fig. 10(b))

Given $\Delta A^{(1)} = 0$ $\Delta A^{(2)} = 0.20$ in.

$\Delta\varphi_2$ eq. (19) Geom I: 18' 13"

Geom II: 14' 23"

Kinematic Errors Due to Gear Eccentricity

Since for eccentric gears the kinematic error function $\Delta\varphi_2(\varphi_1)$ changes from tooth to tooth, one must take into account which tooth of the gear is in mesh. Specifically, φ_1^* denotes the total angle of rotation of the pinion and is the value to be used in equation (22) where φ_1 appears. Here

$$\varphi_1^* = (n-1)\ \frac{360^\circ}{N_1} + \frac{\varphi_A}{\sin \gamma_1}$$

$$\varphi_2 = \varphi_1^*/M_{12}$$

where $n = 1, 2, \ldots, N_1$ is the pinion tooth number being considered and φ_2 is the total angle of rotation of the gear.

Given $\gamma_1 = \gamma_2 = 0$

$\Delta e_1 = 0.002$ in.

$\Delta e_2 = 0$

For $\varphi_A = 1.3419^\circ$, $N = 4$, $\varphi_1 = 57^\circ$, $\varphi_2 = 28.5^\circ$, and applying equations (20) and (21) (see figs. 11(a) and (b))

$\Delta\varphi_2$ = Geom I: -1' 32"

= Geom II: -1' 29"

For the smooth kinematic error function, apply eqations (22) and (23), such that

$a_1 = -1.5395 \times 10^{-3}$ in. $\quad b_1 = 1.2963 \times 10^{-4}$ in.

$a_2 = 0.0$ $\quad b_2 = 0$

Using equation (22) with $\varphi_1 = 57^\circ$ results in (fig. 11(c))

$\Delta\varphi_2 = -1'\ 31"$

REFERENCES

1. Litvin, F., Theory of Gearing, 2nd Ed., Nauka, 1968 (in Russian).

2. Baxter, M., "Effect of Misalignment on Tooth Action of Bevel and Hypoid Gears," ASME Paper 61-MD-20, 1961.

3. Townsend, D. P., Coy, J. J., and Hatvani, B. R., "OH-58 Helicopter Transmission Failure Analysis," NASA TM X-71867, Jan. 1976.

4. Litvin, F. L., Coy, J. J., and Rahman, P., "Two Mathematical Models of Spiral Bevel Gears Applied to Lubrication and Fatigue Life," International Symposium on Gearing and Power Transmissions, Vol. 1, Tokyo, 1981, pp. 281-286.

5. Litvin, F., et al., "Precision of Gear Trains," NASA TM-82887; AVRADCOM TR-C-10, 1982.

6. "Assembling Bevel and Hypoid Gears," AGMA Standard 333.01, 1969.

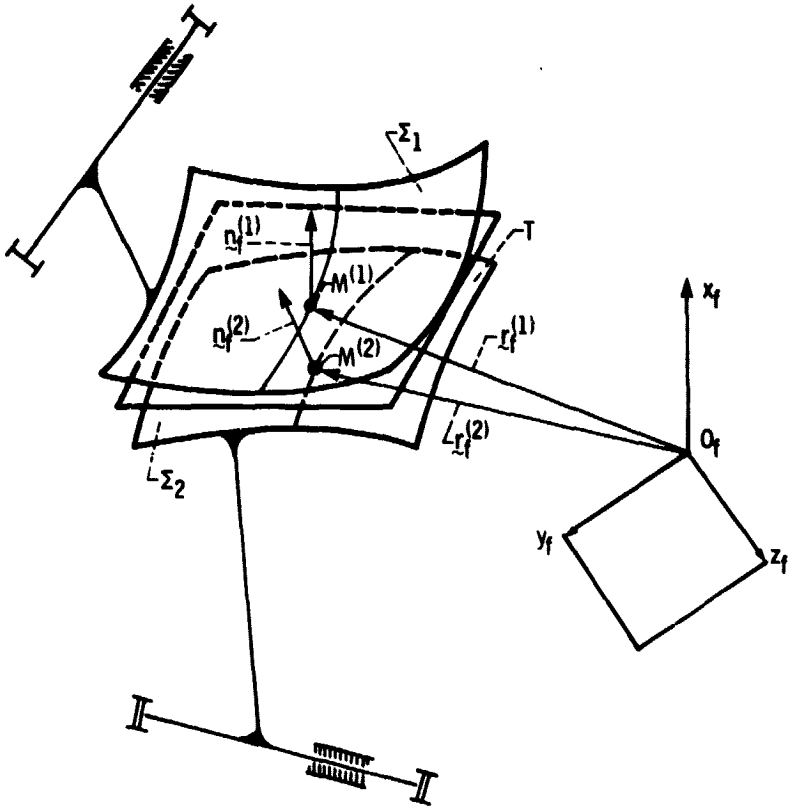

Figure 1. - Tooth surfaces with clearance induced by errors.

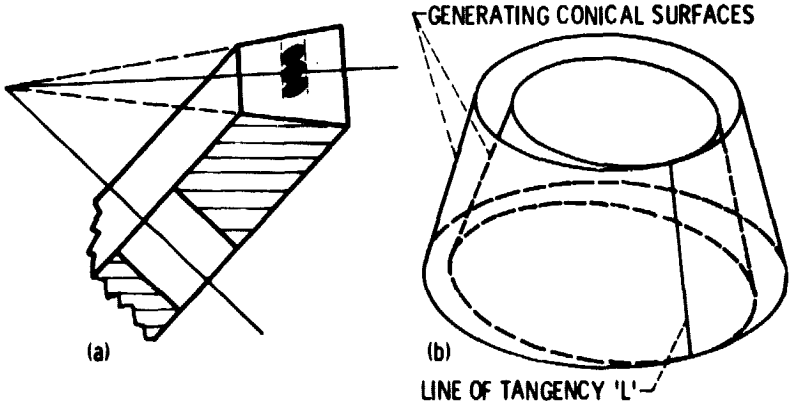

Figure 2. - Geometry I: bearing contact and generating surfaces.

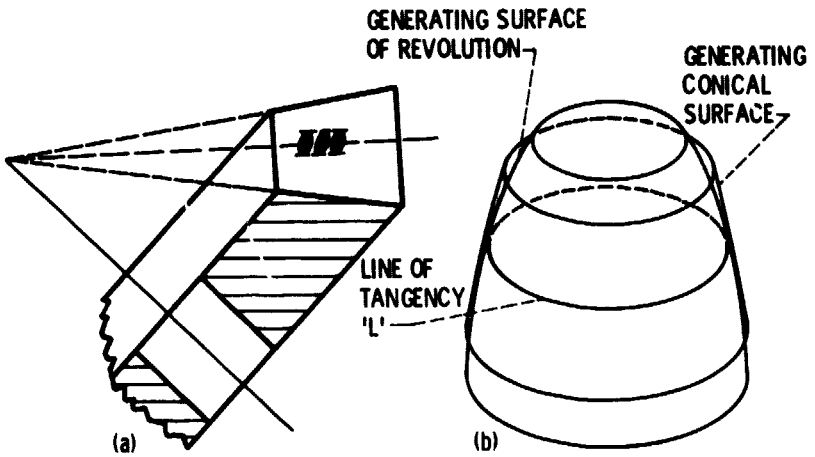

Figure 3. - Geometry II: bearing contact and generating surfaces.

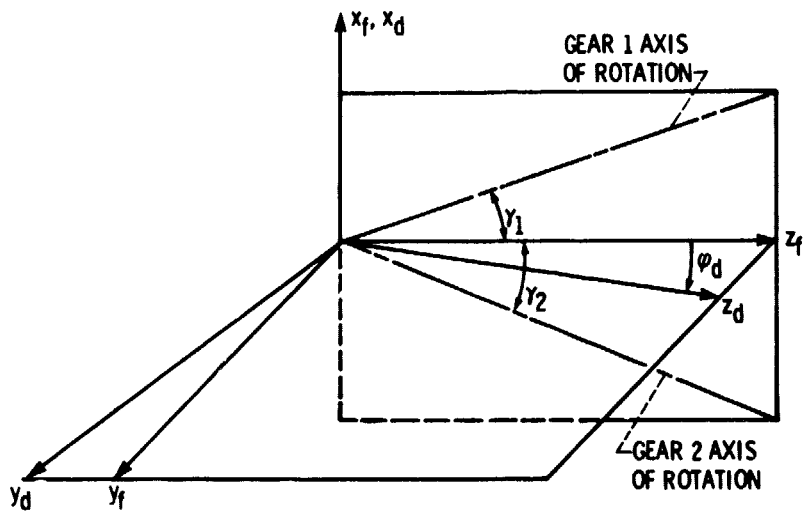

Figure 4. - Applied coordinate systems.

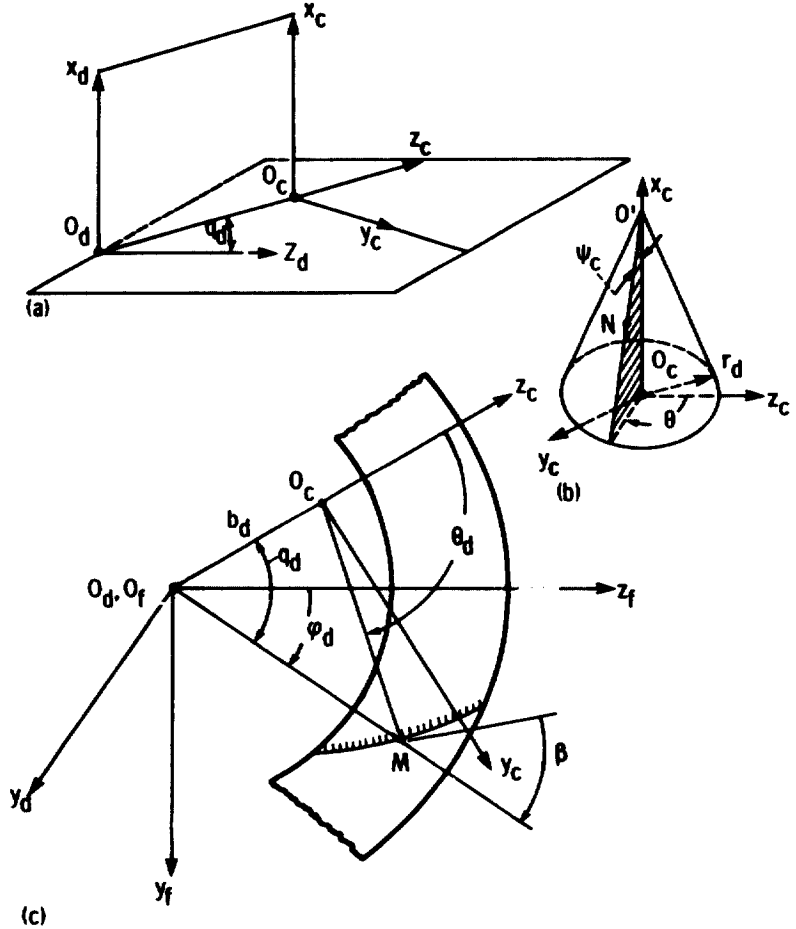

Figure 5. - Applied coordinate systems.

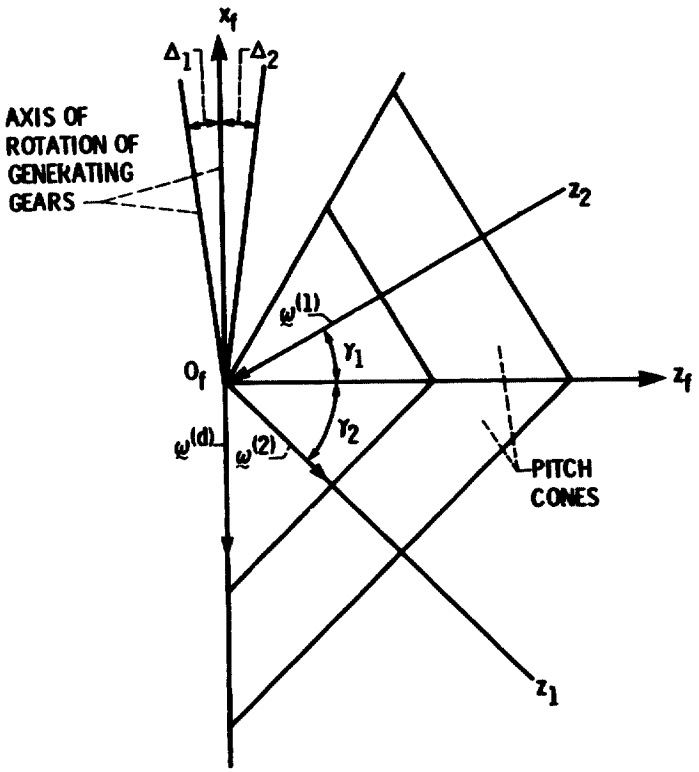

Figure 6. - Axis of rotation of generating gear and member gear.

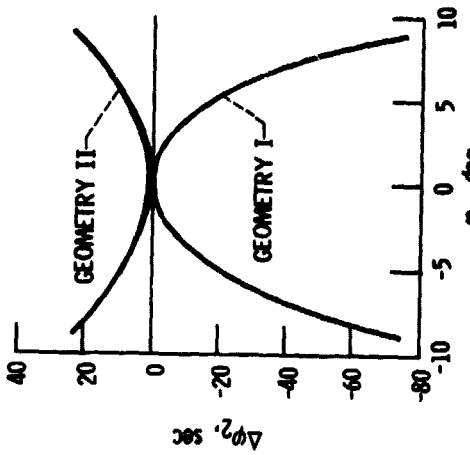

Figure 8. - Kinematic error function due to manufacture with special machine settings.

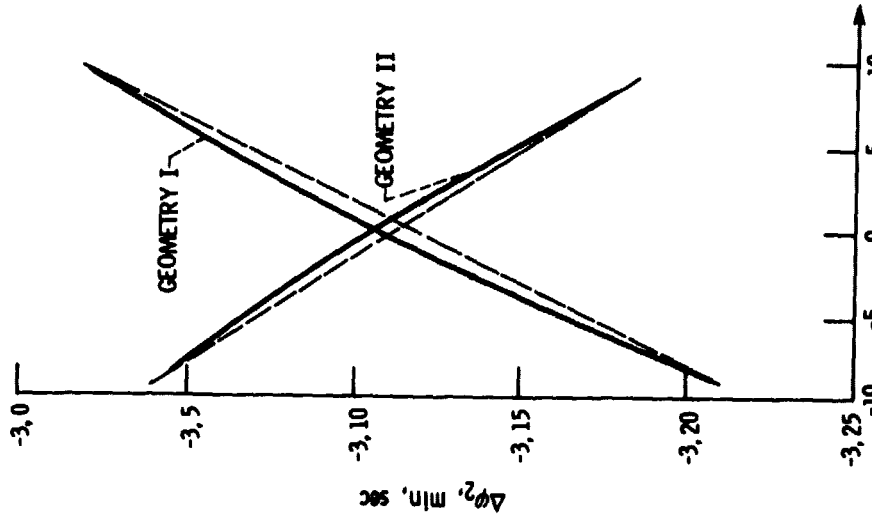

Figure 7. - Kinematic error function due to manufacture without special machine settings.

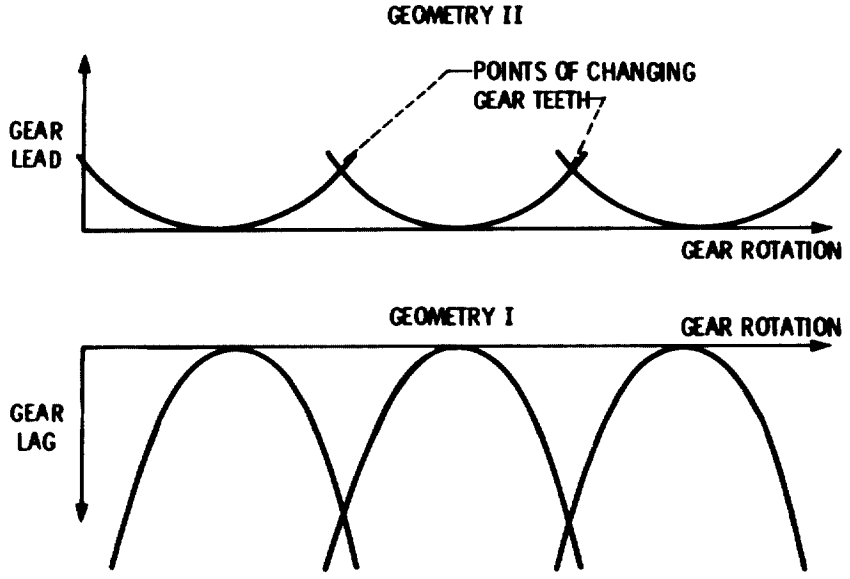

Figure 9. - Kinematic error function for the mesh of several gear teeth.

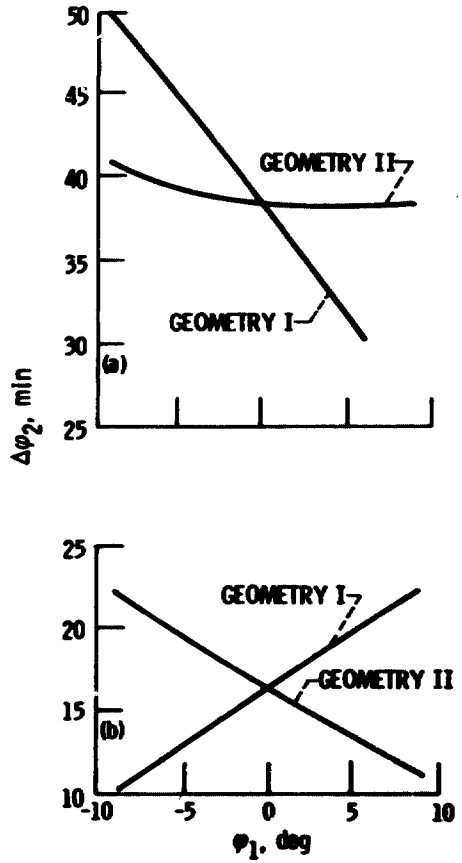

(a) Pinion

(b) Gear

Figure 10. - Kinematic error functions due to axial pinion/gear displacements.

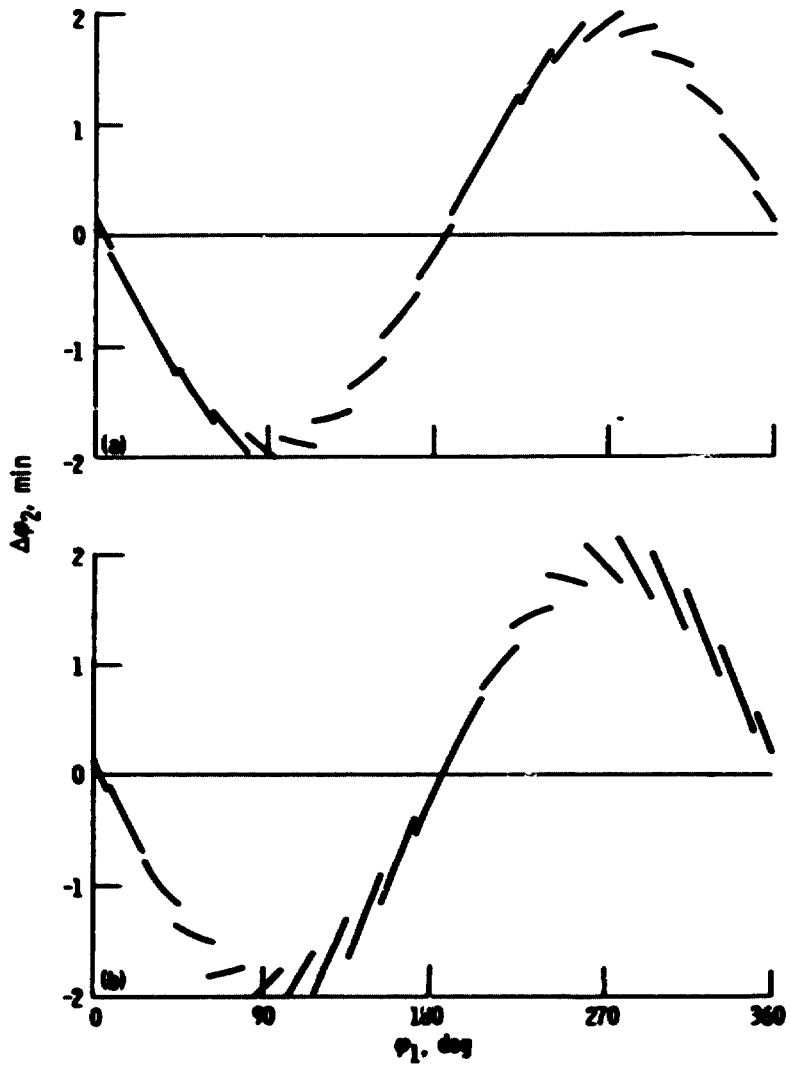

(a) Geometry I.

(b) Geometry II.

Figure 11. - Kinematic error functions due to pinion eccentricity.

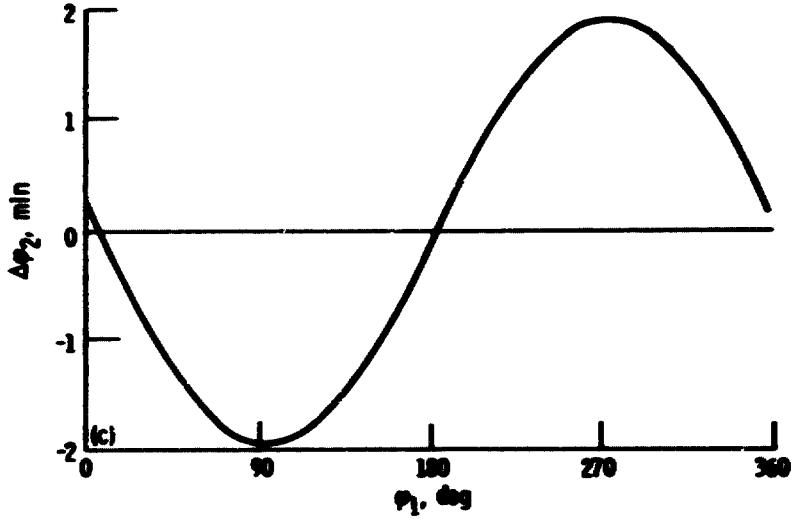

(c) Smooth function.

Figure 11. - Concluded.

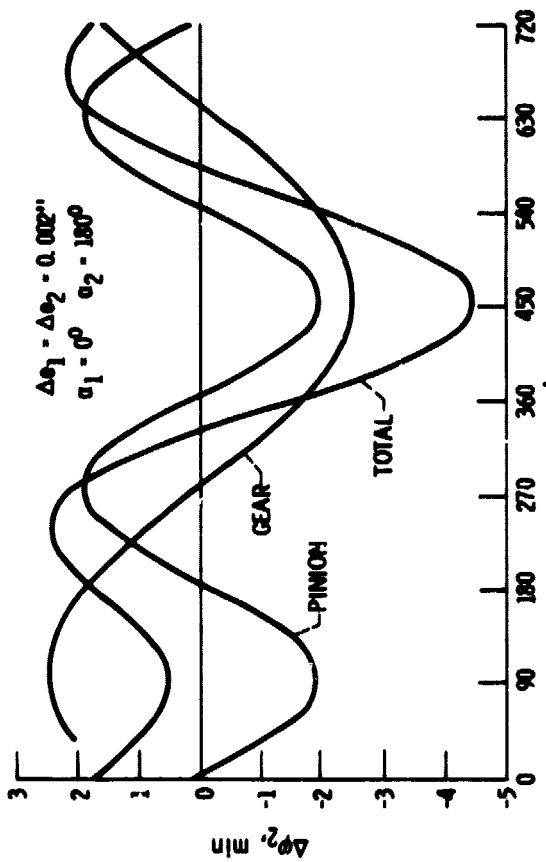

Figure 12. - Kinematic error function due to pinion and gear eccentricity.